First published December 3, 2013; doi:10.1152/ajpendo.00394.2013.

# Hepatocyte growth factor regulates neovascularization in developing fat pads

**Heather M. White,[1] Anthony J. Acton,[1] Malgorzata M. Kamocka,[2] and Robert V. Considine[1]**

[1]*Division of Endocrinology, Department of Medicine, Indiana University School of Medicine, Indianapolis, Indiana; and* [2]*Division of Nephrology, Department of Medicine, Indiana University School of Medicine, Indianapolis, Indiana*

Submitted 16 July 2013; accepted in final form 25 November 2013

**White HM, Acton AJ, Kamocka MM, Considine RV.** Hepatocyte growth factor regulates neovascularization in developing fat pads. *Am J Physiol Endocrinol Metab* 306: E189–E196, 2014. First published December 3, 2013; doi:10.1152/ajpendo.00394.2013.—In this study, we used lentiviral-delivered shRNA to generate a clonal line of 3T3-F442A preadipocytes with stable silencing of hepatocyte growth factor (HGF) expression and examined the long-term consequence of this modification on fat pad development. HGF mRNA expression was reduced 94%, and HGF secretion 79% ($P < 0.01$), compared with preadipocytes treated with nontargeting shRNA. Fat pads derived from HGF knockdown preadipocytes were significantly smaller ($P < 0.01$) than control pads beginning at 3 days postinjection (0.022 ± 0.003 vs. 0.037 ± 0.004 g), and further decreased in size at *day 7* (0.015 ± 0.004 vs. 0.037 ± 0.003 g) and *day 14* (0.008 ± 0.002 vs. 0.045 ± 0.007 g). Expression of the endothelial cell genes *TIE1* and *PECAM1* increased over time in control fat pads (1.6 ± 0.4 vs. 11.4 ± 1.7 relative units at *day 3* and *14*, respectively; $P < 0.05$) but not in HGF knockdown fat pads (1.1 ± 0.5 vs. 5.9 ± 2.2 relative units at *day 3* and *14*). Contiguous vascular structures were observed in control fat pads but were much less developed in HGF knockdown fat pads. Differentiation of preadipocytes to mature adipocytes was significantly attenuated in HGF knockdown fat pads. Fat pads derived from preadipocytes with knockdown of the HGF receptor c-MET were smaller than control pads at *day 3* postinjection (0.034 ± 0.002 vs. 0.049 ± 0.004 g; $P < 0.05$), and remained the same size through *day 14*. c-MET knockdown fat pads developed a robust vasculature, and preadipocytes differentiated to mature adipocytes. Overall these data suggest that preadipocyte-secreted HGF is an important regulator of neovascularization in developing fat pads.

neovascularization; 3T3-F442A; TIE-1; PECAM-1; peroxisome proliferator-activated receptor-γ; lipoprotein lipase

THERE IS INTENSE INTEREST in understanding the function of the adipose tissue vasculature in health and disease. It is known that angiogenesis is required to support the substantial growth potential of adipose tissue and that angiogenesis plays a critical role in the development of obesity (8, 20, 31). On the other hand, a number of studies have suggested that in obesity the adipose tissue is hypoxic, either due to rarefaction or insufficient blood flow, and that adipose tissue hypoxia is a root cause of the chronic inflammation characteristic of obesity (28, 31). In related areas of inquiry, studies to understand adipocyte-regulated vascular growth are expected to provide novel insight into the mechanisms responsible for the greater risk of cancer in obese subjects (27), and there continues to be an active interest in targeting the adipose tissue vasculature as a means of treating and/or preventing obesity (5, 13, 34).

Our laboratory is investigating the role of hepatocyte growth factor (HGF), a potent angiogenic and mitogenic factor, in the regulation of adipose tissue vascular growth. We have shown that both adipocytes and preadipocytes secrete HGF, that circulating HGF is elevated in obese humans, and that weight loss decreases HGF (2, 29). Using the 3T3-F442A in vivo fat pad formation model, we previously observed that preadipocyte HGF expression regulates early neovascular events in fat pads that develop following injection of preadipocytes under the skin of BALB/c nude mice (1). In that study we used an electroporation technique to deliver small-interfering RNA (siRNA) targeting HGF into 3T3-F442A cells, achieving a transient 82% knockdown of HGF mRNA and protein secretion. At 72 h postinjection, mRNA for the endothelial cell markers tyrosine kinase with immunoglobulin-like and epidermal growth factor-like domains 1 (TIE1) and platelet endothelial cell adhesion molecule 1 (PECAM1) was significantly reduced in fat pads derived from preadipocytes with HGF knockdown compared with that in fat pads from control preadipocytes. Immunohistochemical staining demonstrated more endothelial cells in the muscle layer next to fat pads derived from control 3T3-F442A cells than in those with HGF knockdown, but neither endothelial cells nor vascular structures were detected by immunohistochemistry in the center of injected preadipocytes. We concluded from these findings that preadipocyte HGF expression was required for early neovascularization of developing fat pads, but a number of questions remained unanswered. The long-term effects of silencing HGF in developing fat pads could not be tested because of the transient nature of the HGF knockdown achieved with electroporated siRNA. The effect of HGF knockdown on the size of developing fat pads was not quantitated, and the formation of mature vascular structures within the fat pad was not observed. Finally, adipocytes express the HGF receptor c-MET (3), and given that an autocrine effect of HGF on cell survival has been observed (15), it remains to be established if loss of autocrine/paracrine signaling to preadipocytes impairs fat pad development.

In the current study, we used lentiviral-delivered short-hairpin loop siRNA to induce stable HGF silencing in 3T3-F442A preadipocytes and examined the long-term consequences on fat pad development. Based on our observations suggesting that preadipocyte HGF knockdown had acute effects on vascular recruitment to the developing fat pad, we hypothesized that establishment of viable fat pads containing mature adipocytes would be inhibited when derived from preadipocytes lacking HGF. We also hypothesized that loss of autocrine HGF signaling via c-MET in preadipocytes would not impair fat pad development to the same degree as loss of HGF.

## MATERIALS AND METHODS

*Silencing HGF and c-MET expression.* 3T3-F442A preadipocytes at ~70% confluence were treated with lentiviral shRNA reagents

Address for reprint requests and other correspondence: R. V. Considine, Indiana Univ. School of Medicine, 541 North Clinical Dr., Clinical Bldg. 455, Indianapolis, IN 46202-5111 (e-mail: rconsidi@iupui.edu).

targeting either murine HGF or c-MET, or with a scrambled shRNA that did not match any mouse gene, following the manufacturer's protocol (Mission TRC shRNA Lentiviral Target Set; Sigma Aldrich, St. Louis, MO). After selection with puromycin, surviving clones were screened for mRNA knockdown. Of the five HGF-targeted lentiviral clones tested, maximal knockdown was achieved with clone TRCN0000031279 (CCGGCCTGAAGATACTTGAATGAATCTCGAGATTCATTCAAGTATCTTCAGGTTTTTG). Clone TCN0000-0023531 (CCGGCCCGACGTGAACACATTTGATCTCGAGATCAAATGTGTTCACGTCG) targeting c-MET provided the best knockdown of this target gene. The selected preadipocyte lines were expanded in DMEM + 10% bovine calf serum (BCS), and aliquots were frozen.

*Cell culture.* Preadipocytes were maintained in DMEM + 10% BCS. For differentiation culture medium was changed to DMEM + 10% fetal bovine serum with 10 μg/ml insulin (Sigma-Aldrich) for 8 days. HGF secretion from cultured cells was measured using a mouse-specific HGF ELISA (Raybiotech, Norcross, GA). Secretion was normalized to cell DNA on the dish determined using the PicoGreen dsDNA kit (Life Technologies, Grand Island, NY).

*Western blotting.* Membrane-bound proteins were extracted from siNON, siMET, and HEK293 (positive control) cell lysates using the Mem-PER Plus Protein Extraction Kit per the manufacturer's protocol (Thermo Fisher Scientific, Waltham, MA). The protein concentration was determined by BCA protein assay (Pierce, Rockford, IL). Protein lysates (75 μg) and Precision Plus Western C standard with Strep-Tactin horseradish peroxidase (HRP) conjugate secondary antibody (Bio-Rad, Hercules, CA) were separated on a 4–16% gradient gel and transferred to a polyvinylidene fluoride membrane. The membrane was blocked (1× TBS, 0.1% Tween 20, and 5% nonfat dry milk) for 2 h at room temperature and then incubated with mouse monoclonal antibody to Met (ab3127; Cell Signaling Technology, Boston, MA) diluted (1:1,000) in blocking solution overnight at 4°C with gentle shaking. After being washed, the membrane was exposed to donkey anti-mouse IgG-HRP secondary antibody (ab97080; Abcam, Cambridge, MA) diluted (1:5,000) for 1 h at room temperature. The membrane was washed and protein was detected using Super Signal (ThermoScientific, Hanover Park, IL) and visualized by a ChemiDoc (Bio-Rad). Exposure times adequate to visualize Met bands resulted in oversaturation of Western C standard; therefore, ChemiDoc Image Lab software (Bio-Rad) was used to merge the ladder image from a less-exposed capture (10 s) onto a longer-exposed capture (450 s). ChemiDoc Image Lab software (Bio-Rad) was also used for quantification of band intensity. Equivalent protein loading was verified by quantitation of the nonspecific band density at ~70 kDa (siNON: 8,890,880; siMET: 8,854,677; HEK293: 8,757,140).

*Fat pad formation in vivo.* Undifferentiated preadipocytes were trypsinized from the flasks and washed with culture medium. Cells ($1.5 \times 10^7$) in 0.05 ml DMEM + 10% BCS were injected just under the skin on the back of 8- to 10-wk-old male BALB/c athymic nude mice (Charles River Laboratories, Wilmington, MA). Each mouse received an injection of nontargeted preadipocytes (siNON) with either HGF knockdown (siHGF) or c-MET knockdown (siMET) preadipocytes on the opposite side of the spine. In some cases mice received injections of all three types of preadipocytes such that two fat pads were formed on the same side of the spine with one more dorsal and the other more ventral. When growing two fat pads on the same side of the spine, injections were randomized. Animal use was approved by the Indiana University School of Medicine Institutional Animal Care and Use Committee.

*Real-time RT-PCR.* Isolation of RNA, primers for peroxisome proliferator-activated receptor-γ (PPARγ), lipoprotein lipase (LPL), TIE1, and PECAM1, and methods for real-time PCR have been previously described (1) except that an ABI Prism 7300 Sequence Detection System (Applied Biosystems, Foster City, CA) was used for the current study. Primers for murine preadipocyte factor 1 (Pref-1) (30), vascular endothelial growth factor (VEGF) (25), hypoxia-inducible factor-1α (HIF-1α) (19), CD-68 (37), BAX (35), and CHOP (22) were from the literature. Primers for c-MET were forward 5′-GAATGTCGTCCTACACGGCC-3′ and reverse 5′-CACTACACAGTCAGGACACTGC-3′. Gene expression was normalized to 36B4 [mouse acidic ribosomal phosphoprotein (1)] expression using the delta $C_T$ method. There was no difference in 36B4 expression in 3T3-F442A preadipocytes or adipocytes following differentiation in vitro or in vivo.

*Confocal microscopy.* Confocal imaging was performed on growing fat pads to obtain qualitative information on vascular and fat cell development using the method of Nishimura et al. (26). Fat pads were removed and stained with BODIPY 558/568 dodecanoic acid and isolectin G5-IB4 conjugated to Alexa Fluor 488 (Molecular Probes, Life Technologies). Confocal images of whole tissue mounts were acquired with a confocal/two-photon Olympus Fluoview FV-1000 MPE system (Olympus America, Central Valley, PA) available at the Indiana Center for Biological Microscopy facility (Indianapolis, IN), using an Olympus XLUMPLFL 20×, NA 0.95 water-immersion objective. Images were collected in a sequential illumination mode using 488- and 559-nm laser lines while fluorescent emission was collected in two spectral detectors with filter range set up to 500–545 nm for green dye and 570–670 nm for red dye. Series of sections through the depth of tissue (Z-stacks) were collected using optimal step size settings with images comprised of 512 × 512 pixels (634 × 634 $\mu m^2$). Projection images of 33-μm-thick Z-stacks were created using MetaMorph imaging software (Molecular Devices, Downingtown, PA).

*Statistical analyses.* All data are expressed as means ± SE. Statistical comparison of differentiation in vitro was done by paired *t*-test. Comparison of gene expression and protein secretion in the three preadipocyte cell lines, or in fat pads derived from the three cell lines, was done by two-tailed unpaired *t*-test for normally distributed data and by two-tailed Mann-Whitney test for data not normally distributed. Effect of time on fat pad weight and gene expression was assessed by one-way analysis of variance followed by Tukey's Multiple-Comparison Test. Means were considered significantly different when $P < 0.05$. All analyses were done using GraphPad Prism Version 5.

## RESULTS

*Silencing HGF expression impairs fat pad development.* A 3T3-F442A preadipocyte cell line in which HGF expression was silenced (siHGF) was derived by treatment with lentiviral-driven shRNA, antibiotic selection, and cloning using standard techniques. A control preadipocyte cell line (siNON) was derived by identical techniques using a nontargeting lentiviral shRNA. A 94% reduction in HGF mRNA was achieved (0.2 ± 0.01 vs. 2.8 ± 0.6 relative units; $n = 6$; $P < 0.01$). HGF secretion from siHGF preadipocytes in vitro was reduced by 79% compared with siNON preadipocytes (17.7 ± 9.9 vs. 85.2 ± 8.2 ng HGF·μg $DNA^{-1}$·48 $h^{-1}$; $n = 4$, $P < 0.01$). Lentiviral-treated preadipocytes readily differentiated in vitro. In siNON preadipocytes, PPARγ expression increased 9 ± 2-fold (2.4 ± 1.2 to 11.8 ± 3.6 relative units, $n = 7$, $P < 0.02$) and LPL expression increased 11 ± 3-fold (10.0 ± 2.8 to 73.8 ± 7.9 relative units; $P < 0.005$) at *day 8* compared with *day 0*. In siHGF preadipocytes, differentiated in vitro PPARγ expression increased 13 ± 4-fold (0.3 ± 0.1 to 2.5 ± 0.6 relative units, $n = 8$; $P < 0.01$), and LPL expression increased 54 ± 19-fold (1.3 ± 0.3 to 36.1 ± 9.9 relative units; $P < 0.005$).

siNON preadipocytes injected under the skin of nude mice formed readily identifiable fat pads that were contained within a connective tissue pocket, as previously observed (1). The weight of siNON fat pads did not change over the course of the 14-day observation period (Fig. 1). In contrast, siHGF fat pads were significantly smaller ($P < 0.01$) than siNON fat pads

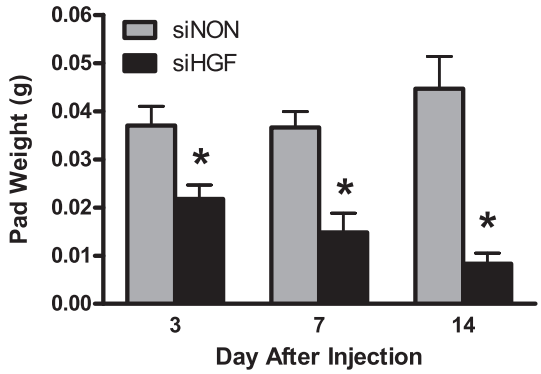


Fig. 1. Lack of preadipocyte hepatocyte growth factor (HGF) expression reduces size of developing fat pads. 3T3-F442A preadipocytes with HGF knockdown (siHGF) and control preadipocytes (siNON) were injected under the skin of nude mice, and developing fat pads were removed and weighed on the indicated day postinjection. Values represent means ± SE for $n = 13$ siNON and siHGF fat pads at *day 3*; $n = 7$ siNON and 5 siHGF fat pads at *day 7* (2 siHGF pads not found); and $n = 13$ siNON and 9 siHGF fat pads at *day 14* (4 siHGF pads not found). $^{*}P < 0.01$ compared with siNON fat pad at that time point.

beginning at *day 3*, with siHGF fat pad size continuing to decrease over time. At 7 days postinjection, siHGF fat pads could not be identified in two of seven mice. At 14 days fat pads could not be found in 4 of 13 siHGF-injected mice. The mean weight of the siHGF fat pads shown in Fig. 1 was calculated using only the weight of fat pads recovered at each time point.

Markers of preadipocyte differentiation to mature adipocytes increased over time in siNON fat pads. PPARγ and LPL expression was significantly greater ($P < 0.05$) at 14 days compared with that at 3 days (Fig. 2). In contrast, expression of PPARγ and LPL in siHGF fat pads did not increase over time, and was significantly less ($P < 0.02$) than that of siNON fat pads at all times, indicating a failure of the preadipocytes to differentiate in vivo. Expression of the preadipocyte marker Pref-1 decreased in siNON fat pads by *day 14*. Pref-1 was higher in siHGF fat pads and did not change over the course of the experiment.

Expression of the endothelial cell-specific genes TIE-1 and PECAM-1 increased over time in fat pads from siNON preadipocytes such that expression at *day 14* was significantly greater than that at *day 3* (Fig. 3). In siHGF fat pads, TIE-1 mRNA expression did not differ over time and was significantly less ($P < 0.05$) than that in siNON fat pads at *day 14*. PECAM-1 expression in siHGF fat pads increased over time but remained significantly less than that in siNON fat pads at *day 14*. Confocal microscopic images of a representative siNON and siHGF fat pad are shown in Fig. 4. A contiguous vasculature and large lipid-filled adipocytes are readily noted in the siNON fat pad. In contrast, endothelial cell staining is detectable in the siHGF fat pad, but functional capillaries do not appear to be present. Some lipid-filled adipocytes are present, but these are smaller and much fewer in number than in the control fat pad.

To probe possible mechanisms through which loss of preadipocyte HGF resulted in impaired fat pad development, we examined expression of several additional genes in fat pads at 72 h postinjection. HIF-1α was significantly greater in siHGF than siNON fat pads (Fig. 5). There was no difference in expression of VEGF (9.5 ± 1.5 vs. 9.4 ± 1.3), CD68 (17.9 ± 4.4 vs. 19.4 ± 4.4), CHOP (9.6 ± 0.9 vs. 9.3 ± 1.5), or BAX (2.5 ± 0.3 vs. 2.8 ± 0.1 relative units) between siNON and siHGF fat pads at 3 days postinjection.

*Preadipocytes with reduced HGF receptor c-MET expression form fat pads.* A 3T3-F442A preadipocyte cell line in which c-MET expression was knocked down (siMET) was derived by the same procedures used to knockout HGF expression. A 40% reduction in c-MET mRNA was achieved (1.3 ± 0.2 vs. 2.2 ± 0.4 relative units; $n = 6$; $P < 0.05$), which decreased c-MET protein 44% (Fig. 6). HGF secretion from siMET preadipocytes in vitro was increased to 280% of that from siNON preadipocytes (239.0 ± 4.4 vs. 85.2 ± 8.2 ng HGF·μg $DNA^{-1}$·48 $h^{-1}$; $n = 4$, $P < 0.01$). In siMET preadipocytes differentiated in vitro, PPARγ expression increased

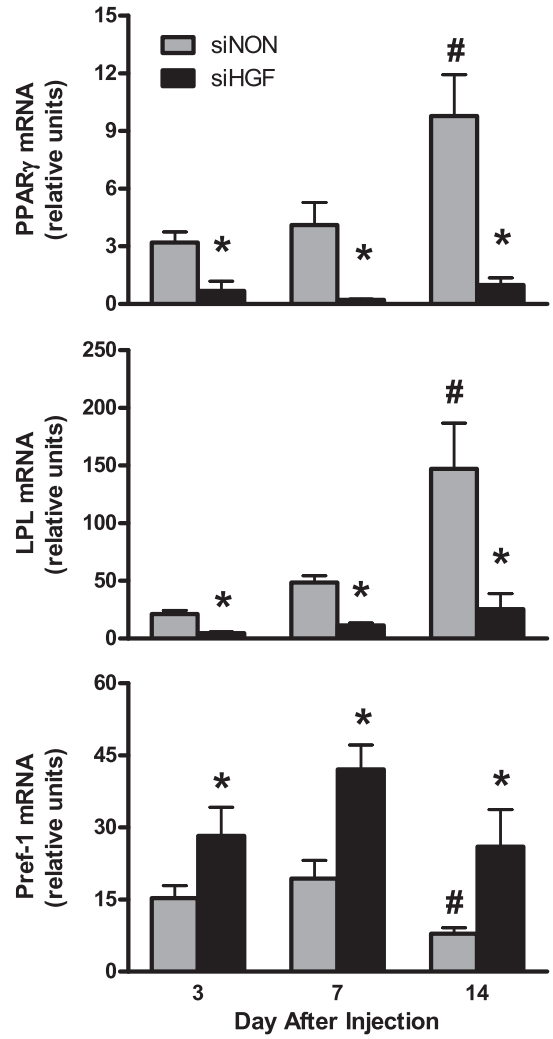


Fig. 2. Inhibition of preadipocyte HGF expression impairs differentiation to mature adipocytes in vivo. In siNON fat pads, expression of adipocyte markers peroxisome proliferator-activated receptor-γ (PPARγ) and lipoprotein lipase (LPL) is greater at *day 14* compared with *day 3*, and expression of the preadipocyte marker preadipocyte factor 1 (Pref-1) mRNA is less at *day 14* than *day 3*. In siHGF fat pads, markers of adipocyte maturity do not increase with time and are significantly less than that in siNON fat pads. Pref-1 in siHGF fat pads is greater than that in siNON fat pads all time points and does not decrease over time. Values represent means ± SE for the no. of fat pads described in Fig. 1. $^{\#}P < 0.05$ compared with *day 3* fat pad; $^{*}P < 0.02$ compared with siNON fat pad at that time point.

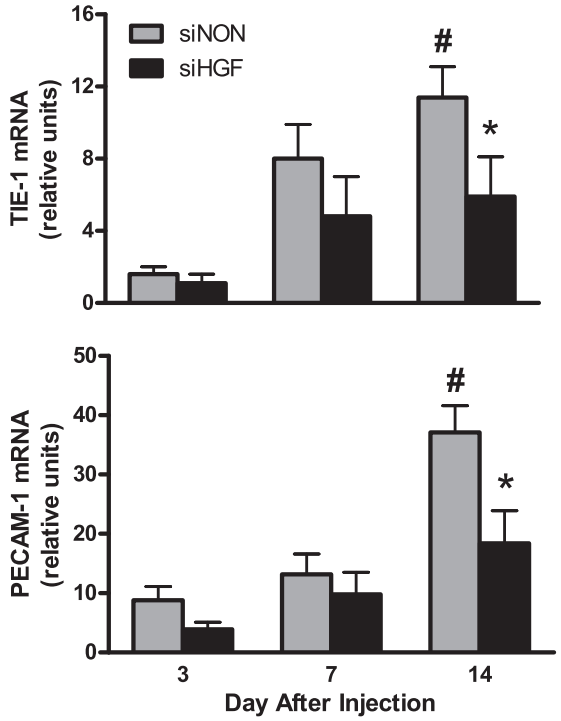


Fig. 3. Markers of endothelial cell migration into developing fat pads are reduced with silencing of preadipocyte HGF expression. In siNON fat pads, the expression of tyrosine kinase with immunoglobulin-like and epidermal growth factor-like domains 1 (TIE-1) and platelet endothelial cell adhesion molecule 1 (PECAM-1) is greater at *day 14* compared with *day 3*. Expression of TIE-1 and PECAM-1 in siHGF fat pads is significantly less than in siNON fat pads at *day 14*. Values represent means ± SE for the no. of fat pads described in Fig. 1. $^{\#}P < 0.05$ compared with *day 3* fat pad; $^{*}P < 0.05$ compared with siNON fat pad at that time point.

109 ± 37-fold (0.04 ± 0.01 to 3.9 ± 1.8 relative units, $n = 8$, $P < 0.001$), and LPL expression increased 72 ± 25-fold (2.7 ± 1.5 to 50.8 ± 6.1 relative units; $P < 0.001$).

In this series of experiments, the size of siNON fat pads was significantly larger at *day 14* than *day 7* (Fig. 7). In contrast to the effect of HGF knockdown to result in progressively smaller fat pads, the weight of siMET fat pads did not change over the 14-day time period. However, siMET fat pad weight was significantly less ($P < 0.05$) than that of the siNON fat pads at *day 3* and *day 14* (Fig. 7).

In both siNON and siMET fat pads PPARγ and LPL expression increased over time and was significantly greater ($P < 0.05$) at 14 days compared with that at 3 days (Fig. 8). Expression of PPARγ and LPL in siMET pads was significantly less than that in siNON fat pads ($P < 0.05$) at most time points, which might be explained by the lower expression of these transcription factors in siMET preadipocytes before injection (see above in vitro differentiation data). Despite lower levels in siMET preadipocytes, PPARγ expression in siMET fat pads increased 55 ± 17-fold from *day 3* to *day 14* compared with a 5 ± 1-fold increase in siNON pads ($P < 0.05$). The fold increase in LPL expression in siMET fat pads was similar to that in siNON fat pads (11 ± 4 vs. 20 ± 7; $P > 0.05$). In both siNON and siMET fat pads Pref-1 decreased over time such that expression at *day 14* was significantly less than that at *day 3*. Pref-1 was higher in siMET fat pads than in siNON fat pads at all time points.

As shown in Fig. 9 expression of TIE-1 and PECAM-1 increased over time ($P < 0.05$) in fat pads from both siNON and siMET preadipocytes. Importantly, TIE-1 and PECAM-1 mRNA expression in siMET fat pads was not different from that of siNON fat pads. Vascular structures and lipid-filled adipocytes were present in siMET fat pads at 14 days postinjection (Fig. 4).

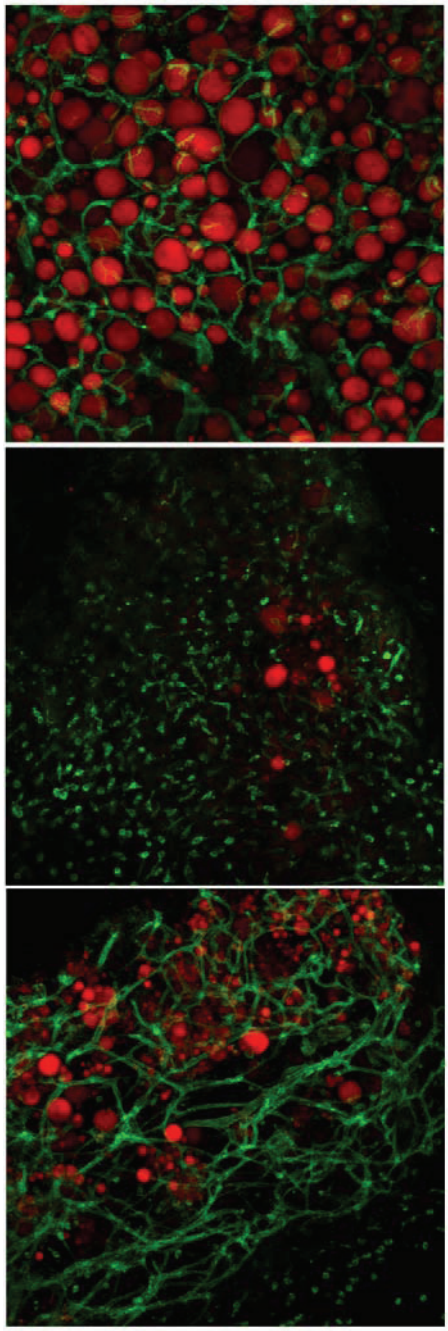

Fig. 4. Confocal imaging of developing fat pads. Unfixed fat pads at 14 days postinjection were stained with BODIPY (red) for fatty acid and isolectin (green) for endothelial cells. Note the large adipocytes and well-developed vasculature in the siNON fat pad (*top*). In contrast, mature adipocytes and contiguous vascular structures were absent in the siHGF fat pad (*middle*). Fat pads derived from preadipocytes with silencing of c-MET expression (siMET) showed a well-developed vasculature and mature adipocytes (*bottom*).

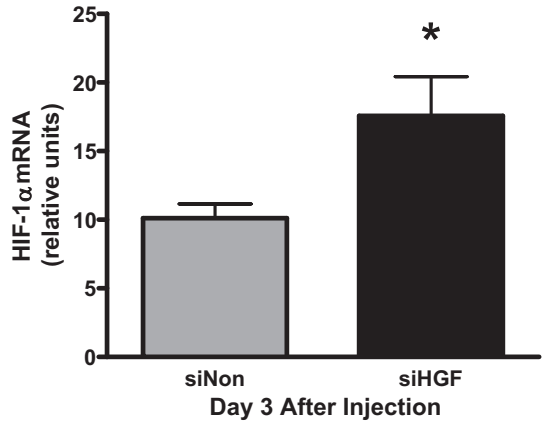


Fig. 5. Hypoxia-inducible factor-1α (HIF-1α) expression is greater in fat pads derived from siHGF preadipocytes at 3 days postinjection. Values represent means ± SE for 13 siNON and 13 siHGF fat pads. *$P < 0.05$ compared with siNON fat pad at that time point.

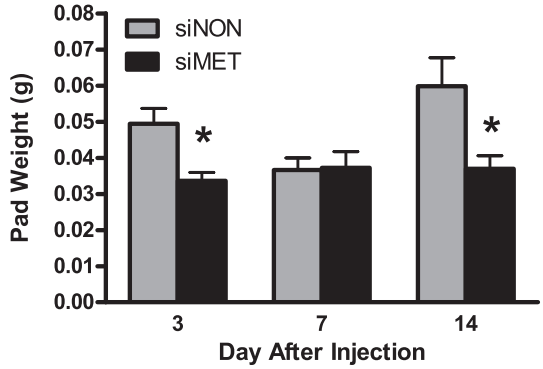


Fig. 7. Preadipocytes with knockdown of c-MET expression (siMET) form viable fat pads. siNON and siMET preadipocytes were injected under the skin of nude mice, and developing fat pads were removed and weighed on the indicated day postinjection. Note that siMET fat pad weight is stable across the 14-day experimental period. Values represent means ± SE for $n = 7$ siNON and siMET fat pads at *day 3* and *14*, with $n = 7$ siNON and 6 siMET fat pads at *day 7* (1 siMET pad not found). *$P < 0.02$ compared with siNON fat pad at that time point.

## DISCUSSION

Understanding the basic mechanisms regulating vascular growth in adipose tissue is needed to better address the metabolic dysregulation that occurs in obesity. HGF is an important angiogenic factor in adipose tissue, facilitating communication between preadipocytes, adipocytes, and endothelial cells. In the present study we provide novel insight into the role of preadipocyte HGF to promote vascular growth. Using the 3T3-F442A in vivo fat pad formation model we show that, in the absence of preadipocyte HGF, mature fat pads fail to develop because of impaired neovascularization, resulting in hypoxia and attenuation of preadipocyte differentiation to mature adipocytes. A reduction in autocrine HGF signaling, achieved by knockdown of HGF receptor c-MET expression, did not impair fat pad development.

When injected under the skin of nude mice, 3T3-F442A preadipocytes differentiate into mature adipocytes in a fat pad contained within a connective tissue pocket (1, 9, 23, 25). Using fluorescently labeled preadipocytes, we have observed that fat pads are derived from the injected cells (data not shown), in agreement with the observations of Mandrup et al. (23) using 3T3-F442A preadipocytes expressing nuclear β-galactosidase. These investigators further found that preadipocytes are not proliferating at 1, 2, or 4 wk after implantation, suggesting that clonal expansion/proliferation occurs within the first 5 days following injection under the skin. Neels et al. (25) confirmed that preadipocytes do not differentiate into endothelial cells and that the neovasculature of the developing fat originates by sprouting from host-derived blood vessels.

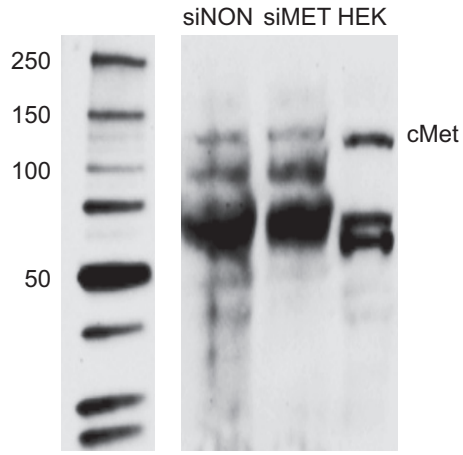


Fig. 6. Membrane c-MET protein is reduced in preadipocytes with silencing of c-MET expression. Relative band density: siNON = 1,045,520; siMET = 592,098; HEK = 2,107,784. HEK-293 cells (HEK) run as a positive control with high c-MET expression.

In the present study, lentiviral-treated and clonally selected preadipocytes with unaltered HGF expression (siNON) readily formed fat pads in vivo, and the weight of these fat pads at *day 3* and *14* was not different. In early work with this model, other investigators described, but did not document by measuring weight or volume, that fat pads looked smaller after injection under the skin, then steadily became much larger at 4–6 wk postinjection (16, 23). Our data in Fig. 7, derived from independent fat pads excised at each time point, support the concept that fat pads can become smaller and then expand in size. Mechanisms that could contribute to smaller fat pads in the period immediately after injection include loss of fluid volume from in and around the injected cells, closer packing of cells as extracellular matrix forms, and resorption of the necrotic core in the center of injected cell mass (25). Conversely, increases in fat pad size should result from clonal expansion of differentiating preadipocytes and accumulation of lipid within mature adipocytes. Data in both Figs. 1 and 7 suggest that siNON fat pads were trending larger by *day 14* than *day 3*. Longer time points postinjection (4–6 wk) would be needed to definitively establish if fat pads become larger over time under the conditions in our laboratory.

Preadipocytes in siNON fat pads differentiated into mature adipocytes with significant increases in expression of PPARγ and LPL. Message levels for TIE-1 and PECAM-1, previously shown to correlate with histological evidence of endothelial cells in developing fat pads (1, 25), concomitantly increased as preadipocyte differentiation occurred. Finally, confocal imaging at *day 14* confirmed the presence of mature lipid-filled adipocytes and contiguous vascular structures in siNON fat pads. These observations are in agreement with earlier work

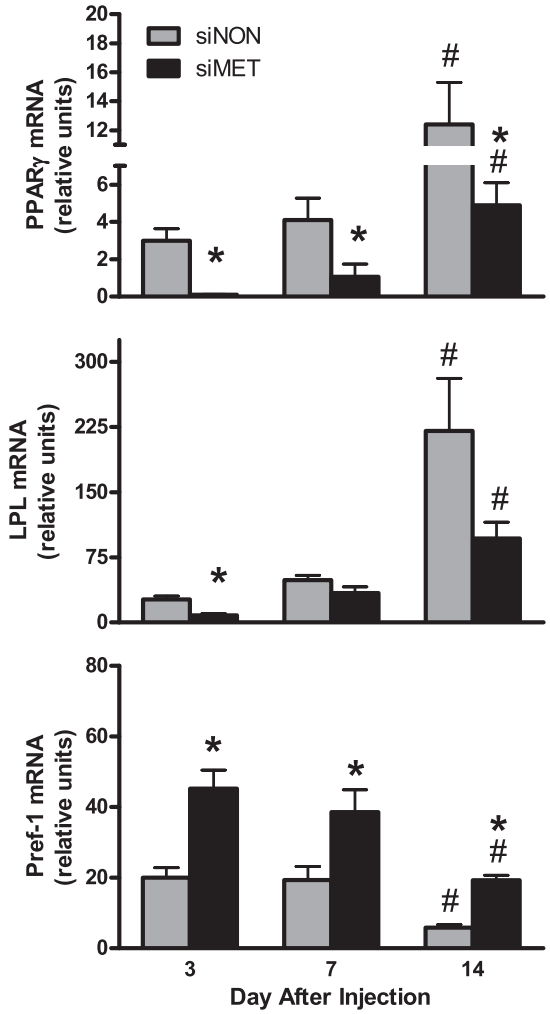


Fig. 8. Increased adipocyte differentiation over time in fat pads derived from preadipocytes with c-MET knockdown. In both siNON and siMET fat pads, expression of adipocyte markers PPARγ and LPL is greater at *day 14* compared with *day 3*. PPARγ expression in siMET fat pads increased 55 ± 17-fold from *day 3* to *day 14* compared with a 5 ± 1-fold increase in siNON pads. The fold increase in LPL expression in siMET fat pads was similar to that in siNON fat pads (11 ± 4 vs. 20 ± 7; $P > 0.05$). Values represent the means ± SE for the no. of fat pads described in Fig. 7. $^{\#}P < 0.05$ compared with *day 3* fat pad; $^{*}P < 0.05$ compared with siNON fat pad at that time point.

documenting that angiogenesis and adipogenesis are interdependent events in development and growth of adipose tissue (12, 17, 18).

Fat pads derived from siHGF preadipocytes were smaller than siNON fat pads beginning at *day 3* and continued to decrease in size across the experimental period. Expression of PPARγ and LPL in siHGF fat pads was low but, more importantly, did not significantly increase over time. In vitro, expression of PPARγ and LPL increased 13- and 54-fold, respectively, during differentiation of siHGF preadipocytes, ruling out defects due to lentiviral knockdown of HGF. In contrast, differentiation in vivo was significantly impaired, with the lack of mature lipid-filled adipocytes contributing to the smaller size of siHGF fat pads. TIE-1 and PECAM-1 expression was detectable in siHGF fat pads, and confocal microscopy confirmed that endothelial cells were present; however, a functional vascular network had not formed by *day 14*. These observations support our hypothesis that HGF is needed for proper vascular development and that preadipocyte differentiation depends on a functional vasculature. In support of this interpretation, Fukumura et al. (14) observed that blocking angiogenesis with an anti-VEGF receptor antibody impaired differentiation of 3T3-F442A preadipocytes in a dorsal skin fold chamber model.

Hypoxia inhibits differentiation of 3T3-L1 and 3T3-F442A preadipocytes in vitro by promoting/maintaining expression of Pref-1 (6, 21), a well-established inhibitor of the differentiation process (32) that has also recently been shown to inhibit preadipocyte proliferation (24, 33). Hypoxia was greater in siHGF fat pads at 3 days postinjection as indicated by greater HIF-1α expression. Pref-1 was significantly greater in siHGF fat pads than in siNON fat pads at all time points and did not change over the 14-day experimental period. Thus, in the absence of preadipocyte HGF, impaired neovascularization resulted in hypoxia and maintenance of Pref-1 expression, which inhibited clonal expansion and differentiation of preadipocytes.

We noted that 4 of the 13 siHGF fat pads initiated were not found by *day 14*, suggesting that siHGF preadipocytes did not survive. Measures of endoplasmic reticulum stress (CHOP), initiation of apoptosis (BAX), and macrophage markers (CD68) were not different between siHGF and siNON fat pads, providing no evidence for programmed cell death. Neels et al. (25) provided histological evidence for resorption of the necrotic core within the developing fat pad, and preadipocytes can exhibit phagocytic properties similar to that of macro-

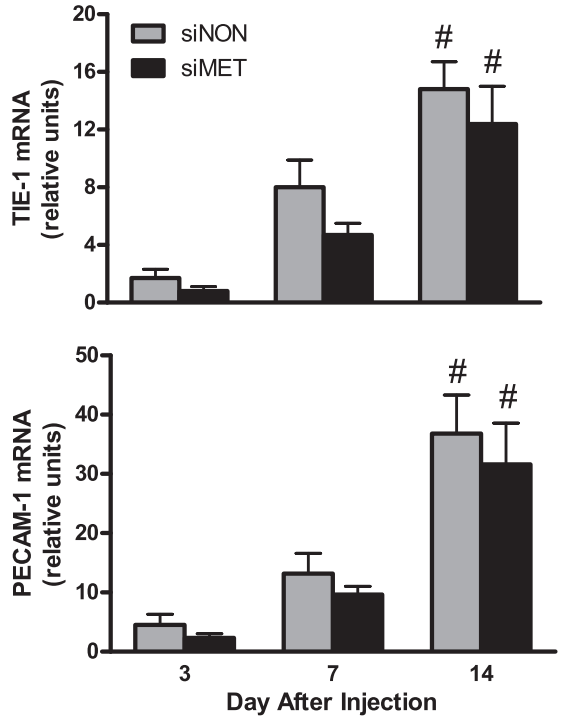


Fig. 9. The increase in endothelial cell markers over time in fat pads derived from preadipocytes with c-MET knockdown is the same as that in fat pads from control preadipocytes. In both siNON and siMET fat pads, expression of TIE-1 and PECAM-1 is greater at *day 14* compared with *day 3*. Values represent means ± SE for the no. of fat pads described in Fig. 7. $^{\#}P < 0.05$ compared with *day 3* fat pad.

phages (7, 10, 11). Thus it is possible that siHGF preadipocytes became necrotic and were resorbed. Alternatively, preadipocytes may have been difficult to see and physically separate from the host tissue because they had not undergone clonal expansion to increase cell number, or differentiated and filled with lipid. Future studies employing siHGF preadipocytes with a visual tag or stain will be needed to fully address this possibility.

HGF is not only a potent angiogenic factor acting on endothelial cells but also promotes growth and survival of other cell types (15). Preadipocytes express the HGF receptor c-MET, and HGF has been shown to stimulate glucose uptake in 3T3-L1 adipocytes (3). Furthermore, in a study injecting adipose-derived stem cells with HGF knockdown into ischemic hind limbs, it was noted that loss of HGF expression reduced survival of the injected cells (4). Thus we addressed the question whether autocrine/paracrine HGF signaling was required for fat pad development.

At 3 days postinjection, fat pads derived from siMET preadipocytes were smaller than siNON fat pads. However, in contrast to the progressive decrease in size observed with siHGF fat pads, the weight of the siMET fat pads remained constant over the 14-day experiment. PPARγ, LPL, TIE-1, and PECAM-1 expression increased over time, and Pref-1 decreased over time, indicating that preadipocytes were differentiating and endothelial cells were migrating into the developing fat pad. Confocal microscopy confirmed the presence of mature adipocytes and capillary structures, indicating that loss of autocrine/paracrine HGF signaling in preadipocytes did not significantly impair development of functional fat pads. The finding that Pref-1 was greater in siMET than siNON fat pads suggests that preadipocytes remained or that adipocytes were not fully mature, which may have contributed to the slightly smaller size of the siMET fat pads. A difference in extracellular matrix formation, size of the necrotic core, or amount of lipid contained in the mature adipocytes may also have contributed to smaller siMET fat pads.

It is important to note that c-MET protein was only reduced 44%. Thus it is possible that greater c-MET knockdown may have revealed a larger role for autocrine HGF signaling in fat pad development. siMET preadipocytes also secreted greater amounts of HGF than did siNON or siHGF preadipocytes, possibly because of loss of feedback with reduced c-MET abundance. Increased HGF secretion may have had a compensatory effect to promote fat pad development in these experiments.

We have previously shown that adipocytes from obese humans secrete more HGF than adipocytes from lean subjects (2), and observations in the current study provide strong evidence for preadipocyte HGF to promote vascular development in adipose tissue. Given these findings, it is not clear why adipose tissue HGF does not prevent hypoxia or rarefaction in obesity. One possibility is that cytokines or other factors in the adipose tissue act on the endothelial cells to block the effect of HGF to promote or maintain vascular development in obesity. An alternate hypothesis is that elevated HGF in adipose tissue of obese subjects has a strong protective effect on the vasculature, and that, if this angiogenic factor were not present, vascular defects and hypoxia would be even more pronounced. Transgenic mouse models with adipose tissue-specific knockout of HGF expression will be needed to fully address this point.

Two limitations of this study deserve mention. We demonstrated that silencing HGF expression impaired fat pad development but did not do functional rescue by transfection to restore HGF expression. However, we did use a scrambled shRNA control cell line to account for the effects of lentiviral treatment and antibiotic selection. Furthermore, targeting c-MET did not impair development of fat pads as observed when targeting HGF, strengthening the likelihood that effects were specific to HGF knockdown. Second, we could not fully differentiate between inhibition of clonal expansion and resorption of necrotic preadipocytes as the main cause for progressively smaller, and in some cases absent, siHGF fat pads. Future experiments with lineage-specific tags and direct measures of preadipocyte proliferation will be needed to fully resolve the fate of siHGF preadipocytes.

In summary, our data strongly support a role for HGF in the regulation of adipose tissue vascular growth. We show that loss of preadipocyte HGF expression significantly attenuates neovascularization in developing fat pads, resulting in impaired differentiation of preadipocytes to mature adipocytes. Loss of autocrine HGF signaling did not impair development of functional fat pads. Understanding the interaction of preadipocytes and adipocytes with the adipose tissue vasculature should provide important insight into the mechanisms contributing to metabolic dysregulation in obesity.

## ACKNOWLEDGMENTS

Current address for H. M. White: Dept. of Dairy Science, Univ. of Wisconsin-Madison, 1675 Observatory Dr., Rm. 934B, Madison, WI 53706.

## GRANTS

This work was supported by NIH grant R01 DK081574-01.

## DISCLOSURES

No conflicts of interest, financial or otherwise, are declared by the authors. RV Considine is a Consultant for Merck on gastrointestinal hormones which is not the topic of this manuscript.

## AUTHOR CONTRIBUTIONS

Author contributions: H.M.W. and R.V.C. conception and design of research; H.M.W., A.J.A., M.M.K., and R.V.C. performed experiments; H.M.W., A.J.A., M.M.K., and R.V.C. analyzed data; H.M.W., A.J.A., M.M.K., and R.V.C. interpreted results of experiments; H.M.W., M.M.K., and R.V.C. prepared figures; H.M.W. and R.V.C. drafted manuscript; H.M.W., A.J.A., M.M.K., and R.V.C. edited and revised manuscript; H.M.W., A.J.A., M.M.K., and R.V.C. approved final version of manuscript.

## REFERENCES

1. **Bell LN, Cai L, Johnstone BH, Traktuev DO, March KL, Considine RV.** A central role for hepatocyte growth factor in adipose tissue angiogenesis. *Am J Physiol Endocrinol Metab* 294: E336–E344, 2008.
2. **Bell LN, Ward JL, Degawa-Yamauchi M, Bovenkerk JE, Jones RM, Cacucci BM, Gupta CE, Sheridan C, Sheridan K, Shankar SS, Steinberg HO, March KL, Considine RV.** Adipose tissue production of hepatocyte growth factor contributes to elevated serum HGF in obesity. *Am J Physiol Endocrinol Metab* 291: E843–E848, 2006.
3. **Bertola A, Bonnafous S, Cormont M, Anty R, Tanti JF, Tran A, Marchand-Brustel YL, Gual P.** Hepatocyte growth factor induces glucose uptake in 3T3–L1 adipocytes through a GAB1/PI3-kinase/GLUT4 pathway. *J Biol Chem* 282: 10325–10332, 2007.
4. **Cai L, Johnstone BH, Cook TG, Liang Z, Traktuev D, Cornetta K, Ingram DA, Rosen ED, March KL.** Suppression of hepatocyte growth factor production impairs the ability of adipose-derived stem cells to

promote ischemic tissue revascularization. *Stem Cells* 25: 3234–3243, 2007.
5. **Cao Y.** Adipose tissue angiogenesis as a therapeutic target for obesity and metabolic diseases. *Nat Rev Drug Discov* 9: 107–115, 2010.
6. **Carrière A, Carmona MC, Fernandez Y, Rigoulet M, Wenger RH, Pénicaud L, Casteilla L.** Mitochondrial reactive oxygen species control the transcription factor CHOP-10/GADD153 and adipocyte differentiation: a mechanism for hypoxia-dependent effect. *J Biol Chem* 279: 40462–40469, 2004.
7. **Charrière G, Cousin B, Arnaud E, André M, Bacou F, Penicaud L, Casteilla L.** Preadipocyte conversion to macrophage. Evidence of plasticity. *J Biol Chem* 278: 9850–9855, 2003.
8. **Christiaens V, Lijnen HR.** Angiogenesis and development of adipose tissue. *Mol Cell Endocrinol* 318: 2–9, 2010.
9. **Christiaens V, Van Hul M, Lijnen HR, Scroyen I.** CD36 promotes adipocyte differentiation and adipogenesis. *Biochim Biophys Acta* 1820: 949–956, 2012.
10. **Cousin B, Munoz O, Andre M, Fontanilles AM, Dani C, Cousin JL, Laharrague P, Casteilla L, Pénicaud L.** A role for preadipocytes as macrophage-like cells. *FASEB J* 13: 305–312, 1999.
11. **Cousin B, André M, Casteilla L, Pénicaud L.** Altered macrophage-like functions of preadipocytes in inflammation and genetic obesity. *J Cell Physiol* 186: 380–36l, 2001.
12. **Crandall DL, Hausman GJ, Kral JG.** A review of the microcirculation of adipose tissue: anatomic, metabolic, and angiogenic perspectives. *Microcirculation* 4: 211–232, 1997.
13. **Daquinag AC, Zhang Y, Kolonin MG.** Vascular targeting of adipose tissue as an anti-obesity approach. *Trends Pharmacol Sci* 32: 300–307, 2011.
14. **Fukumura D, Ushiyama A, Duda DG, Xu L, Tam J, Krishna V, Chatterjee K, Garkavtsev I, Jain RK.** Paracrine regulation of angiogenesis and adipocyte differentiation during in vivo adipogenesis. *Circ Res* 93: 88–97, 2003.
15. **Gherardi E, Birchmeier W, Birchmeier C, Vande Woude G.** Targeting MET in cancer: rationale and progress. *Nat Rev Cancer* 12: 89–103, 2012.
16. **Green H, Kehinde O.** Formation of normally differentiated subcutaneous fat pads by an established preadipose cell line. *J Cell Physiol* 101: 169–171, 1979.
17. **Hausman GJ, Richardson RL.** Cellular and vascular development in immature rat adipose tissue. *J Lipid Res* 24: 522–532, 1983.
18. **Hausman GJ, Richardson RL.** Adipose tissue angiogenesis. *J Anim Sci* 82: 925–934, 2004.
19. **He Q, Gao Z, Yin J, Zhang J, Yun Z, Ye J.** Regulation of HIF-1α activity in adipose tissue by obesity-associated factors: adipogenesis, insulin, and hypoxia. *Am J Physiol Endocrinol Metab* 300: E877–E885, 2011.
20. **Lee MJ, Wu Y, Fried SK.** Adipose tissue remodeling in pathophysiology of obesity. *Curr Opin Clin Nutr Metab Care* 13: 371–376, 2010.
21. **Lin Q, Lee YJ, Yun Z.** Differentiation arrest by hypoxia. *J Biol Chem* 281: 30678–30683, 2006.
22. **Lipson KL, Fonseca SG, Ishigaki S, Nguyen LX, Foss E, Bortell R, Rossini AA, Urano F.** Regulation of insulin biosynthesis in pancreatic beta cells by an endoplasmic reticulum-resident protein kinase IRE1. *Cell Metab* 4: 245–254, 2006.
23. **Mandrup S, Loftus TM, MacDougald OA, Kuhajda FP, Lane MD.** Obese gene expression at in vivo levels by fat pads derived from s.c implanted 3T3–F442A preadipocytes. *Proc Natl Acad Sci USA* 94: 4300–4305, 1997.
24. **Mortensen SB, Jensen CH, Schneider M, Thomassen M, Kruse TA, Laborda J, Sheikh SP, Andersen DC.** Membrane-tethered delta-like 1 homolog (DLK1) restricts adipose tissue size by inhibiting preadipocyte proliferation. *Diabetes* 61: 2814–2822, 2012.
25. **Neels JG, Thinnes T, Loskutoff DJ.** Angiogenesis in an in vivo model of adipose tissue development. *FASEB J* 18: 983–995, 2004.
26. **Nishimura S, Manabe I, Nagasaki M, Hosoya Y, Yamashita H, Fujita H, Ohsugi M, Tobe K, Kadowaki T, Nagai R, Sugiura S.** Adipogenesis in obesity requires close interplay between differentiating adipocytes, stromal cells, and blood vessels. *Diabetes* 56: 1517–1526, 2007.
27. **Park J, Euhus DM, Scherer PE.** Paracrine and endocrine effects of adipose tissue on cancer development and progression. *Endocr Rev* 32: 550–570, 2011.
28. **Pasarica M, Sereda OR, Redman LM, Albarado DC, Hymel DT, Roan LE, Rood JC, Burk DH, Smith SR.** Reduced adipose tissue oxygenation in human obesity: evidence for rarefaction, macrophage chemotaxis, and inflammation without an angiogenic response. *Diabetes* 58: 718–725, 2009.
29. **Rehman J, Considine RV, Bovenkerk JE, Li J, Slavens CA, Jones RM, March KL.** Obesity is associated with increased levels of circulating hepatocyte growth factor. *J Am Coll Cardiol* 41: 1408–1413, 2003.
30. **Ronis MJ, Sharma N, Vantrease J, Borengasser SJ, Ferguson M, Mercer KE, Cleves MA, Gomez-Acevedo H, Badger TM.** Female mice lacking p47phox have altered adipose tissue gene expression and are protected against high fat-induced obesity. *Physiol Genomics* 45: 351–366, 2013.
31. **Rutkowski JM, Davis KE, Scherer PE.** Mechanisms of obesity and related pathologies: the macro- and microcirculation of adipose tissue. *FEBS J* 276: 5738–5746, 2009.
32. **Sul HS.** Pref-1: role in adipogenesis and mesenchymal cell fate. *Mol Endocrinol* 23: 1717–1725, 2009.
33. **Traustadottir GA, Kosmina R, Sheikh SP, Jensen CH, Andersen DC.** Preadipocytes proliferate and differentiate under the guidance of Delta-like 1 homolog (DLK1). *Adipocyte* 2: 272–275, 2013.
34. **White HM, Acton AJ, Considine RV.** The angiogenic inhibitor TNP-470 decreases caloric intake and weight gain in high-fat fed mice. *Obesity (Silver Spring)* 20: 2003–2009, 2012.
35. **Xu C, Lu C, Hua L, Jin H, Yin L, Chen S, Qian R.** Rhythm changes of clock genes, apoptosis-related genes and atherosclerosis-related genes in apolipoprotein E knockout mice. *Can J Cardiol* 25: 473–479, 2009.
36. **Ye J.** Adipose tissue vascularization: its role in chronic inflammation. *Curr Diab Rep* 11:203–10, 2011.
37. **Zhang H, Wang Y, Zhang J, Potter BJ, Sowers JR, Zhang C.** Bariatric surgery reduces visceral adipose inflammation and improves endothelial function in type 2 diabetic mice. *Arterioscler Thromb Vasc Biol* 31: 2063–2069, 2011.